Acta Cryst E CRYSTALLOGRAPHIC COMMUNICATIONS

ISSN 2056-9890

Bis(catecholato-κ^2O,O')bis(dimethyl sulfoxide-κO)titanium(IV)

Nisansala Hewage,[a] Carolyn Mastriano,[a] Christian Brückner[a]* and Matthias Zeller[b]

[a]Department of Chemistry, University of Connecticut, Storrs, CT 06269-3060, USA, and [b]Department of Chemistry, Purdue University, 560 Oval Drive, West Lafayette, IN, 47907-2084, USA. *Correspondence e-mail: c.bruckner@uconn.edu

Received 23 February 2022
Accepted 8 March 2022

Edited by J. Reibenspies, Texas A & M University, USA

Keywords: transition-metal catecholates; heteroleptic catecholates; titanium catecholates; crystal structure.

CCDC reference: 2157170

Supporting information: this article has supporting information at journals.iucr.org/e

Bis(benzene-1,2-diolato-κ^2O,O')bis(dimethyl sulfoxide-κO)titanium(IV), $[Ti(C_6H_4O_2)_2(C_2H_6OS)_2]$, crystallizes with two crystallographically independent molecules in the space group $P2_1/c$ emulating orthorhombic $Pbca$ symmetry (β = 90.0445 (9)°]. The two molecules are related by pseudo-glide symmetry, broken by modulation of each one catecholate and dimethyl sulfoxide (DMSO) ligand. Twinning by pseudomerohedry was observed [twin ratio 0.5499 (7):0.4401 (7)]. Complex **3** was obtained by heating of diprotonated titanium tris-catecholate precursor $\mathbf{2^H}$ in DMSO, by formal displacement of a catechol molecule by two DMSO molecules. Complex **3** is just the second heteroleptic, mono-nuclear, neutral bis-catecholate complex with TiO_6 metal coordination, the only other one being its bis-DMF analogue **6**. The two molecules of **3** exhibit a distorted octahedral geometry. The geometry and distortions from ideal symmetry of **3** are discussed and compared to **6** and to cationic tris-catecholate titanium complexes.

1. Chemical context

The dianion of catechol (1,2-dihydroxybenzene, CatH, **1**) is a bidentate, dianionic and non-innocent *O,O*-chelating agent with a particularly high affinity for HSAB hard-metal ions, *i.e.*, ions of high oxidation states or high charge-to-metal-ion-radius ratios (Pierpont & Lange, 1994; Kaim & Schwederski, 2010). Titanium(IV) is one such metal ion and long known to form stable, pseudooctahedral triscatecholate complexes, such as $\mathbf{2^{Et3NH}}$, by reaction of catechol with Ti^{4+} sources under basic conditions (Fig. 1) (Borgias *et al.*, 1984).

Titanium catecholate complexes have found various uses: Titanium triscatecholate complexes of the alkaline earth metals were utilized as molecular precursors to a number of

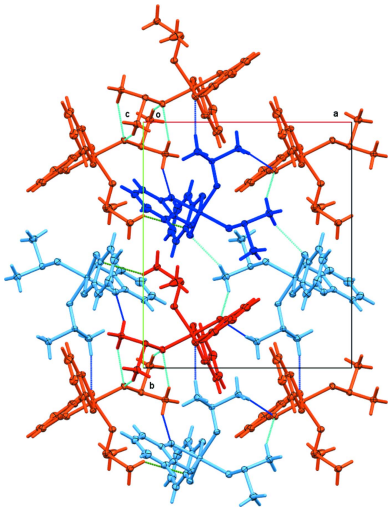

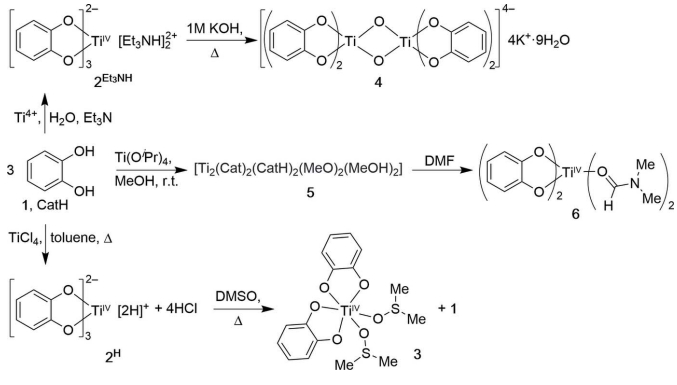

Figure 1
Formation of titanium(IV) catecholate complexes, including the title compound **3**.

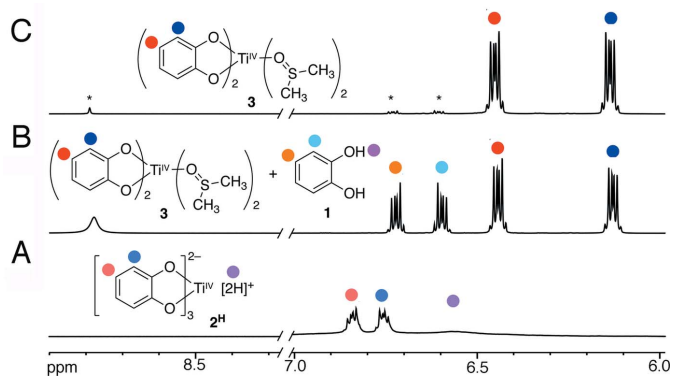

Figure 2
^{1}H NMR spectra (400 MHz, DMSO-d_6) of (*A*) complex $\mathbf{2^H}$ dissolved at ambient temperature; (*B*) of complex $\mathbf{2^H}$ at ∼373 K, showing the presence of complex **3** and free catechol **1**; (*C*) of isolated crystals of **3** precipitated from DMSO at ambient temperature (* indicates the presence of residual **1**).

$M^{II}TiO_6$-type perovskites (Ali & Milne, 1987; Marteel-Parrish *et al.*, 2008). Titanium catecholates have been exploited as catalysts in acetylene hydrogenation (Bazhenova *et al.*, 2016) while three-dimensional titanium catecholate frameworks of high proton conductivity (Nguyen *et al.*, 2015) and titanium catecholate-based MOFs have been described (Cao *et al.*, 2020). Metal catecholates have been suggested as adsorbents for toxic gases (Bobbitt & Snurr, 2018). Titanium tris-catecholates were also used to self-assemble a potential bimodal contrast agent (Dehaen *et al.*, 2012). A number of heteroleptic mono- and multi-nuclear titanium complexes do contain titanium catechol units (Sakata *et al.*, 2010; Bazhenova *et al.*, 2016; Sonström *et al.*, 2019; Passadis *et al.*, 2020) (for further examples, see *Database survey* below). Most prominently, titanium tris-catecholates have been used as versatile building blocks in a range of supramolecular, oligonuclear homo- and hetero-metal-ligand cluster assemblies (Brückner *et al.*, 1998; Caulder *et al.*, 2001; Albrecht *et al.*, 2008, 2019).

Reaction of $TiCl_4$ under anhydrous conditions in toluene generates a brick-colored amorphous powder of the diprotonated titanium tris-catecholate complex $\mathbf{2^H}$ (Davies & Dutremez, 1990). We found that this compound dissolves sufficiently enough in ambient-temperature DMSO-d_6 to record a simple ^{1}H NMR spectrum, showing only two multiplets of equal integration (at 6.84 and 6.75 ppm), corresponding to the *ortho*- and *meta*-hydrogens on three near-identical catecholate moieties (the counter-cations – protons – are believed to be dynamically associated with the trigonal faces of the pseudo-octahedral coordination sphere formed by the six catecholate oxygens) (Fig. 2*A*). Upon heating $\mathbf{2^H}$ in DMSO (or DMSO-d_6), its solubility increases drastically. When followed by ^{1}H NMR spectroscopy, the formation of a new species with two catecholate signals (*m* at 6.42 and 6.12 ppm, in 2:2 intensity) and 1 equivalent of free catechol (*m* at 6.73 and 6.60, *br s* at 8.1 ppm, all 1:1:1) can be observed (Fig. 2*B*). Upon cooling, dark red–orange crystals of the title compound **3** formed. Isolated and analyzed by NMR spectroscopy, they exhibit only the signals for the new species formed (Fig. 2*C*) and the signals for two slightly high-field-shifted DMSO molecules (not shown).

The material was also analyzed by single crystal X-ray diffraction (Fig. 3). Evidently, one protonated catecholate ligand (*i.e.*, catechol **1**) of the starting triscatcholate complex $\mathbf{2^H}$ was exchanged for two DMSO molecules, coordinating through their oxygen atoms in adjacent positions, thus forming a neutral, heteroleptic, mononuclear octahedral complex. Details of the structural arrangement will be discussed in the *Structural commentary* section below.

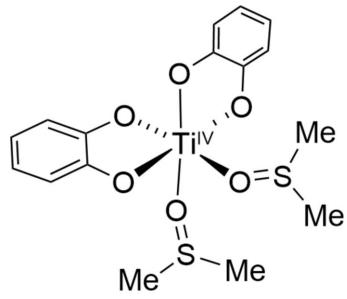

3

The UV–vis spectrum of the orange solution of **3** is overall similar to that of the starting material $\mathbf{2^H}$; both spectra are dominated in the visible range by broad, little-structured catecholate ligand-to-metal charge-transfer bands (for **3**, l_{max} = 441 nm; half-height width > 150 nm; Fig. 4). In comparison to the spectrum of $\mathbf{2^H}$, all bands for **3** are bathochromically shifted.

2. Structural commentary

The title complex **3**, having solution C_2 symmetry, crystallizes as a racemic mixture with two crystallographically independent molecules in the monoclinic space group $P2_1/c$ (Fig. 3).

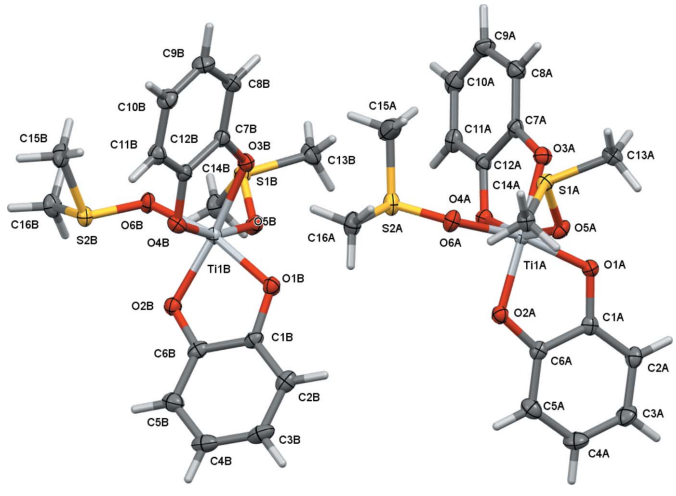

Figure 3
The two crystallographically independent molecules of **3**. View along the *a* axis. Molecules *A* and *B* are related by pseudo-glide operations (see discussion for details).

Table 1
Continuous shape measures (CShM's) relative to ideal reference octahedral symmetry for $\mathbf{2}^{\mathbf{Et3NH}}$, **3** and **6**.

Structure	Hexagon	Pentagonal pyramid	Octahedron	Trigonal prism	Johnson pentagonal pyramid J2
$\mathbf{2}^{\mathbf{Et3NH}}$	33.773	23.482	1.434	9.808	27.215
3A	32.792	22.191	1.491	10.655	26.183
3B	32.830	21.007	1.854	10.159	24.952
6	33.664	22.467	1.513	10.069	26.511

For both molecules, the solution C_2 symmetry is broken in the solid state, and the Ti atoms are each bonded to two chelating catecholate and two monodentate O-coordinated dimethylsulfoxide ligands. The Ti—O_{Cat} bond distances range from 1.9113 (19) to 1.9564 (18) Å in molecule *A*, and 1.9108 (18) to 1.9545 (18) in molecule *B* [average 1.93 (3) Å]. A notable structural *trans*-effect is observed as the longer distances are observed for the oxygen atoms opposite another catechol oxygen donor atom [1.9346 (18) to 1.9564 (18) Å] while the shorter distances [1.9108 (18) to 1.9284 (19) Å] are found *trans* to the weaker electron-donating O_{DMSO} atoms.

The Ti—O_{Cat} bond distances in the cationic triscatecholate complex $\mathbf{2}^{\mathbf{Et3NH}}$ are on average longer [1.97 (3) *vs* 1.93 (3) Å in **3**], ranging from 1.941 (1) to 2.014 (1) Å with differences between long and short Ti—O bonds caused by distortion from strong hydrogen bonds to the Et_3NH^+ counter-cations (reflected in a 0.05 Å lengthening of the associated Ti—O bonds) (Borgias *et al.*, 1984). The four Ti—O_{DMSO} bond distances in **3** are at 2.0214 (19) to 2.0416 (18) Å significantly longer than the Ti—O_{Cat} bond lengths, as would be expected for neutral and uncharged DMSO ligands.

The bond lengths in **3** also compare well with those of the [biscatecholate-bis-DMF]titanium complex **6**, the DMF analogue to the title compound (Bazhenova *et al.*, 2016) and the only other reported heteroleptic mono-nuclear and uncharged bis-catecholate titanium complex with MO_6 metal coordination (see *Database survey*). The Ti—O_{cat} bond lengths in **6** are 1.9003 (12) and 1.9181 (12) Å for the oxygen atoms *trans* to the DMF molecules, 1.9408 (11) and 1.9483 (11) Å when *trans* to another O_{cat} atom, and 2.0396 (12) and 2.0736 (12) Å for the Ti—O_{DMF} bond lengths. They thus closely mirror those found in **3**.

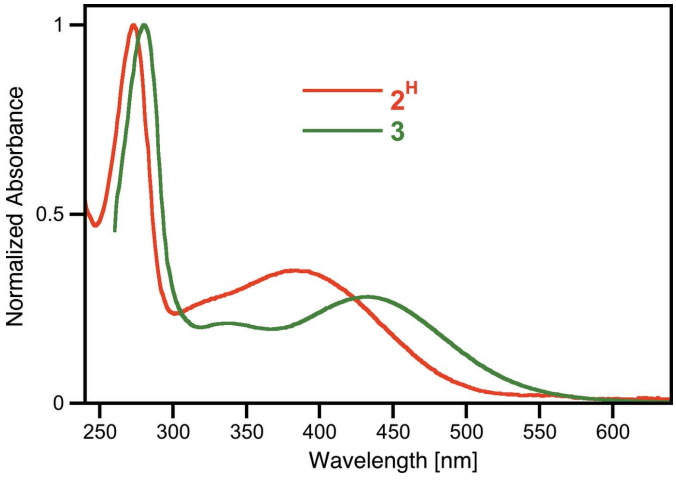

Figure 4
Normalized UV–vis spectrum of title compound **3** (DMSO) in comparison to that of the starting triscatecholate **1** (H_2O).

The small bite angles of the chelating catecholate anions induce substantial distortions from idealized octahedral symmetry. The catecholate O—Ti—O angles in **3** are 80.73 (7) and 81.00 (8)° in molecule *A* and 80.85 (8) and 80.24 (8)° in molecule *B*, which are essentially indistinguishable from those in $\mathbf{2}^{\mathbf{Et3NH}}$ [80.1 (1) to 80.6 (1)°] and **6** [O3 80.68 (5) and O2 80.97 (5)°]. The other *cis* angles in **3** cover a wide range from as small as 82.35 (7)° (for the O_{DMSO}—Ti—O_{DMSO} angle in molecule *A*) to as large as 105.30 (8)° (for one of the O_{cat}—Ti—O_{DMSO} angles in molecule *B*). The latter rather obtuse large angle is unique in being nearly 4° wider than the next largest angle [its equivalent in molecule *A* is 101.66 (8)°]. The angles in $\mathbf{2}^{\mathbf{Et3NH}}$ do not exceed 101.3°. The equivalent angles in the DMF analogue **6** are more evenly distributed than in either molecule of **3**, ranging from 82.53 (5) to 97.77 (5)°.

This more pronounced deviation from ideal octahedral symmetry for molecule *B* of **3** is also confirmed by a more holistic analysis, using a normalized root-mean-square deviation algorithm to calculate the distortion from octahedral symmetry as implemented in the program *SHAPE* (Pinsky & Avnir, 1998; Alvarez *et al.*, 2002; Casanova *et al.*, 2004). The calculated continuous shape measures (CShM's) relative to ideal reference octahedral symmetry are 1.434 for $\mathbf{2}^{\mathbf{Et3NH}}$, 1.513 for **6**, 1.491 for less distorted molecule *A* of **3**, and 1.854 for molecule *B* (Table 1). Shape measures may be between 0 and 100 where zero represents a perfect fit for the selected shape, and CShM values of less than 1.0 are usually interpreted as only minor distortions from the reference shape. Values between 1 and 3 indicate substantial distortions, but the reference shape still provides a good stereochemical description (Cirera *et al.*, 2005). For the four cases analyzed here, the CShM's for the next best fit, trigonal prismatic, are all around 10 (Table 1). The geometries of **3**, **6** and $\mathbf{2}^{\mathbf{Et3NH}}$ are thus best described as distorted octahedral, being far removed from fitting any other polygon.

The two independent molecules in compound **3** are related to each other by crystallographic pseudosymmetry. Complex **3** crystallized in a pseudo-orthorhombic setting with a refined β angle of 90.0445 (9)°, and emulates space group *Pbca* with additional *b*- and *a*-glide operations along the *a*- and *c*-axis directions. Exact translational symmetry is broken by modulation of one of the catecholate and one of the DMSO ligands, as discussed below. The metric pseudosymmetry allows for the

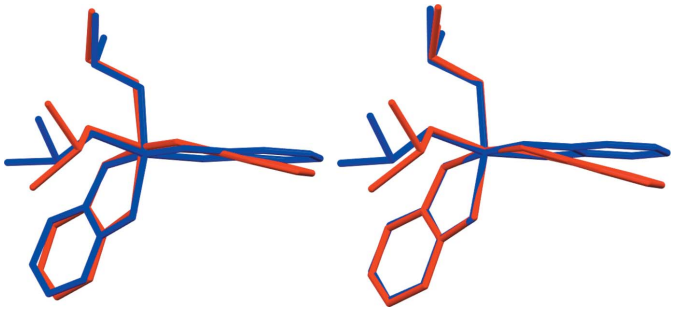

Figure 5
Root-mean-square overlays of the two independent molecules of **3**, after inversion of molecule *B* (red: molecule *A*; blue: molecule *B*). Left: fit based on all non-H atoms (r.m.s. deviation 0.459 Å). Right: fit based on Ti and O atoms only (r.m.s. deviation 0.056 Å).

possibility of twinning. Indeed, the crystal investigated was found to be pseudo-merohedrically twinned by symmetry elements of the emulated orthorhombic symmetry. Application of the twin transformation matrix 1 0 0, 0 −1 0, 0 0 −1 yielded close to equal twin components with a refined twin ratio of 0.5499 (7) to 0.4401 (7).

A root-mean-square overlay of the two molecules yields an r.m.s. deviation of 0.459 Å, indicating substantial variation between the geometries of molecules *A* and *B* (Fig. 5). A similar overlay based on only the titanium and oxygen atoms gives a much smaller value of only 0.056 Å, indicating that the main differences between the two complexes is rooted in the

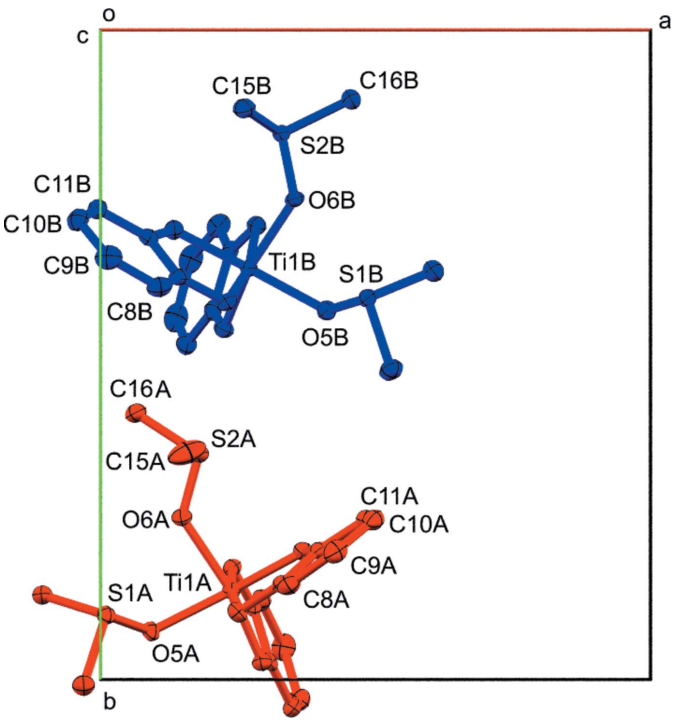

Figure 6
View of **3** down the *c* axis, showing the modulation by pseudo-*Pbca* symmetry. Molecules color coded by symmetry equivalence (red: molecule *A*, blue molecule *B*). Atom labels included for Ti, DMSO S and O atoms, and for C atoms with the largest modulation. 50% probability ellipsoids.

Table 2
Hydrogen-bond geometry (Å, °).

D—H···*A*	*D*—H	H···*A*	*D*···*A*	*D*—H···*A*
C11*A*—H11*A*···O2*B*^{i}	0.95	2.62	3.491 (3)	153
C13*A*—H13*C*···O5*A*^{ii}	0.98	2.54	3.428 (3)	151
C14*A*—H14*B*···O1*A*^{ii}	0.98	2.66	3.378 (3)	130
C14*A*—H14*B*···O5*A*^{ii}	0.98	2.55	3.447 (3)	152
C14*A*—H14*C*···O4*B*^{iii}	0.98	2.27	3.193 (3)	156
C13*B*—H13*E*···O5*B*^{i}	0.98	2.60	3.495 (4)	151
C14*B*—H14*E*···O4*A*^{i}	0.98	2.55	3.438 (3)	151
C14*B*—H14*F*···O1*B*^{i}	0.98	2.56	3.336 (3)	136
C15*B*—H15*D*···O3*A*^{iv}	0.98	2.34	3.307 (3)	171
C16*B*—H16*D*···O1*A*^{iv}	0.98	2.59	3.186 (3)	119
C16*B*—H16*E*···O4*A*^{i}	0.98	2.45	3.427 (3)	173

Symmetry codes: (i) $-x+1, -y+1, -z+1$; (ii) $-x, -y+2, -z+1$; (iii) $-x, -y+1, -z+1$; (iv) $x, y-1, z$.

ligands, even though there are small and noticeable differences for the TiO_6 cores as well (with molecule *B* deviating more from ideal octahedral symmetry than molecule *A*, as discussed above). The main distinction between the two molecules is, however, associated with substantial twists and torsions of the catecholate and DMSO ligands. The r.m.s. overlay reveals a close match of one of the catecholate ligands and one of the DMSO ligands. The other catecholate and DMSO ligands, on the other hand, do show substantial variation between the two molecules. The catecholate of C7–C12 undergoes a twist-motion by a slight rotation around the O_{cat}—O_{cat} axis. In molecule *A* (blue in the overlay), the catecholate ligand is close to coplanar with the titanium atom, while in molecule *B* (red in the overlay) the catecholate and the $TiO(Cat)_2$ plane are clearly angled against each other. The deviations of the Ti atoms from the mean catecholate planes are 0.049 (2) and 0.349 (2) Å for molecules *A* and *B*, respectively. The angle between the mean catecholate and $Ti(OCat)_2$ planes is 1.97 (9)° for complex *A*, but a much larger value of 13.6 (8)° for complex *B*.

The other main difference between the two molecules is a rotation of about 14° for one of the two DMSO ligands around the Ti—O bond, which can be expressed *via* the torsion angle O5—Ti1—O6—S2 (S2 is the sulfur atom of the rotated DMSO ligand, O5 the oxygen atom of the other invariant DMSO ligand). These torsion angles are 165.13 (16)° for molecule *A*, and 151.10 (14)° for molecule *B*. The largest overall motion is observed for the DMSO methyl groups of C15 [1.774 (3) Å in the r.m.s. overlay based on the titanium and oxygen atoms].

The differences in molecular geometry between molecules *A* and *B* and the modulation by pseudo-orthorhombic symmetry are closely related, showing molecules *A* and *B* as they are related to each other by a pseudo *b*-glide perpendicular to (100) (Fig. 6). In addition to the variations in molecular geometry seen in the molecule overlay, a very slight rotation of the entire complex is also observed.

3. Supramolecular features

The most prominent directional interactions in complex **3** are medium strength C—H···O interactions, involving the DMSO

methyl groups as hydrogen-bond donors, and catecholate and DMSO oxygen atoms as the respective acceptors. Hydrogen bonds with C···O distances below 3.50 Å are given in Table 2. Some of these H···O distances are unusually short for C—H···O interactions, with H···O distances as short as 2.27 and 2.34 Å, approaching distances usually only observed for classical hydrogen bonds involving acidic hydrogens. This might indicate stronger than usual interactions with a possibly larger influence on the packing and molecular arrangement in the solid state than usually observed for C—H···O interactions.

When plotting the C—H···O hydrogen bonds (Fig. 7), it becomes evident that the interactions are different for the two molecules, despite their close relationship by a pseudo-glide operation. Interactions involving the less modulated fragments of **3A** and **3B** exhibit similar hydrogen-bonding environments. C13 and C14 of the less-modulated DMSO molecule exhibit the same type of hydrogen bonds to O1, O4 and O5 in neighboring molecules (see Table 2 for symmetry operators and numerical values). The exact bond lengths for C14 vary slightly, a bond to O5 is broken and one to O4 significantly elongated for molecule *B*, but the overall hydrogen-bonding pattern for this DMSO fragment is very similar for both molecules *A* and *B*. This is not the case for the other significantly modulated DMSO molecule. For **3B**, three significant C—H···O interactions are observed, towards O1*A*, O3*A* and O4*A* of neighboring entities. None of these are found for **3A**. All hydrogen-to-oxygen distances are beyond what could be still regarded as attractive and stabilizing. Methyl carbon atom C16*A* is at a distance of 3.128 Å from O1*B*, close enough for a C—H···O hydrogen bond to be suspected, but its hydrogen atoms are rotated such that the H···O distances are > 2.8 Å, and the C—H···O angles are unfavorable at 97.9 and 99.5° (H-atom positions were clearly resolved in difference-density maps and were allowed to rotate to fit the experimental electron density). The shortest distance involving the H atoms of C16*A* is instead towards C1*B* of a neighboring catecholate ring (2.734 Å, shown as a green dashed line in Fig. 7), and C15*A* does not exhibit any H···*X* contacts < 2.8 Å. This clear difference between the hydrogen-bonding interactions of C15 and C16 in the two molecules is clearly related to the modulation that breaks the exact *Pbca* glide symmetry in the structure of **3**. It is not clear whether the ability to form stronger interactions is the cause for the modulation, or whether the modulation causes the differences in intermolecular interactions and the modulation itself is caused by other less-directional forces such as dispersive interactions. Most likely the concerted effects of both modulation and intermolecular interactions reinforcing and stabilizing each other lead to the observed packing of the molecules.

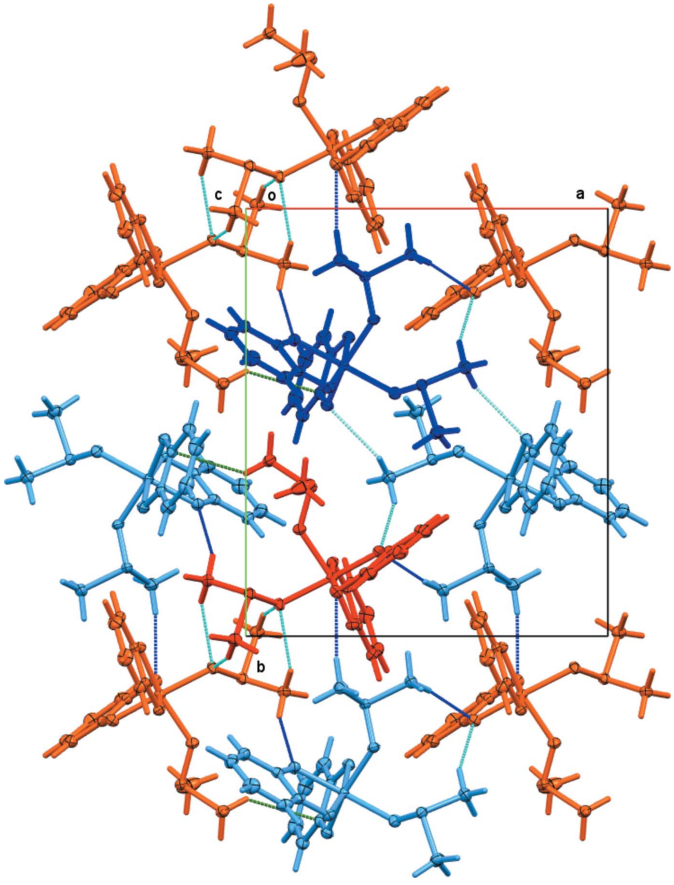

Figure 7
Directional interactions in **3**, viewed down the *c* axis. Red: molecule *A*, blue: molecule *B*. Lighter colored molecules are generated by crystal symmetry. Dark-blue dashed lines: C—H···O bonds with H···O distance < 2.5 Å; light-blue dashed lines: C—H···O bonds with H···O distance between 2.5 and 2.62 A; green dashed lines C—H···π contacts. 50% probability ellipsoids.

4. Database survey

A database survey of titanium catecholate complexes reveals a plethora of homoleptic triscatecholates but only a few in monometallic assemblies. A search of the Cambridge Structural Database (CSD, Version 5.42, accessed Feb 2021; Groom *et al.*, 2016) yields, in addition to $\mathbf{2}^{\mathbf{Et3NH}}$ (Borgias *et al.*, 1984), eleven other monocationic homoleptic triscatecholate titanium complexes with only one metal center: SUKNUK (Kwamen *et al.*, 2020), SUKQAT (Kwamen *et al.*, 2020), GOJMIC (Tinoco *et al.*, 2008), LEXQUD (Dong *et al.*, 2018), LEXRAK (Dong *et al.*, 2018), MAGLAK (Van Craen *et al.*, 2016), VEPJUW (Davis *et al.*, 2006), VEPKAD (Davis *et al.*, 2006), VILXIX (Hahn *et al.*, 1991), XIKLOV (Chen *et al.*, 2018), and YUPNEF (Johnson *et al.*, 2020).

The conversion of triscatecholate complexes to heteroleptic complexes has been observed previously, as the hydroxide-induced displacement of a catecholate ligand from $\mathbf{2}^{\mathbf{Et3NH}}$ to form the bis-(μ-oxo-bridged) biscatecholate **4** exemplifies (Borgias *et al.*, 1984). Direct syntheses are also known (Sakata *et al.*, 2010). For example, treatment of titanium methoxide with a methanolic solution of catechol **1** under ambient conditions resulted in the formation of a dinuclear heteroleptic complex **5** with a mixture of catechol/catecholate and methanol/methanolate ligands (Bazhenova *et al.*, 2016). Notably both examples of these heteroleptic complexes are multinuclear. Complex **5** dissolved in DMF, however, and exchanges all methanol/methanolates for DMF and rearranges to form the mononuclear [biscatecholate-bis-DMF]titanium

complex **6**, the DMF analogue of the title compound (CCDC 1489371; Bazhenova *et al.*, 2016). Neutral and monometallic complexes of this kind are exceedingly rare. A search of the CSD yielded complex **6** as the only other heteroleptic mononuclear, neutral bis-catecholate complex with TiO_6 metal coordination; complex **3** is only the second such complex.

5. Synthesis and crystallization

Triscatcholate $\mathbf{2^H}$ (500 mg, 1.34 × 10 $^{-3}$ mol), prepared as described in the literature (Davies & Dutremez, 1990), was dissolved at ∼173 K, in the minimal amount of DMSO (∼15 ml). The deep, dark-orange solution was allowed to cool slowly (in the water bath) to ambient temperature. The crystal mass that formed was broken up, placed on a porcelain frit, washed with minimal amount of cool DMSO (m.p. 292 K!), then cold diethyl ether, and dried under suction. The red–orange matted plates of **3** (320 mg, 0.76 × 10 $^{-3}$ mol, 57% yield) were analytically pure. By NMR spectroscopy (*cf.* Fig. 3*B*), the reaction is quantitative; nonetheless, no attempt was made to increase the yield by recovery of more product from the filtrate. $C_{16}H_{20}O_6S_2Ti$ (M_W = 420.32 g mol^{-1}); ^{1}H NMR (400 MHz, DMSO-d_6): δ 6.45 (*m*, 2H, 4,5-CH), 6.13 (*m*, 2H, 3,6-CH), 2.31 (*s*, 3H, CH_3) ppm; UV–vis (DMSO): λ_{max} (ε/M^{-1} cm^{-1}) = 280 (9000), 343 (2000), 441 (2500).

6. Refinement

Crystal data, data collection and structure refinement details are summarized in Table 3. The structure exhibits pseudo-orthorhombic symmetry (*Pbca*) and is twinned by a 180° rotation around the *a*- or *c*-axis. Application of the transformation matrix 1 0 0, 0 − 1 0, 0 0 − 1 yielded a twin ratio of 0.5399 (7):0.4401 (7). The pseudo-orthorhombic symmetry is broken by modulation of one of the catecholate rings by up to 1.4 Å, and one of the DMSO ligands by over 1.7 Å.

C—H bond distances were constrained to 0.95 Å for aromatic C—H and to 0.98 Å for aliphatic CH_3 moieties, respectively. U_{iso}(H) values were set to a multiple of U_{eq}(C) with 1.5 for CH_3 and 1.2 for C—H units. Reflections $\bar{1}$12, 112 and 013 were affected by the beam stop and were omitted from the refinement.

Table 3
Experimental details.

Crystal data	
Chemical formula	$[Ti(C_6H_4O_2)_2(C_2H_6OS)_2]$
M_r	420.34
Crystal system, space group	Monoclinic, $P2_1/c$
Temperature (K)	100
a, *b*, *c* (Å)	12.4531 (3), 14.7287 (3), 20.3676 (5)
β (°)	90.0445 (9)
V (Å^3)	3735.78 (15)
Z	8
Radiation type	Mo $K\alpha$
μ (mm^{-1})	0.71
Crystal size (mm)	0.35 × 0.23 × 0.09
Data collection	
Diffractometer	Nonius Kappa CCD
Absorption correction	Multi-scan (*SCALEPACK*; Otwinowski & Minor, 1997)
T_{min}, T_{max}	0.668, 0.939
No. of measured, independent and observed [$I > 2\sigma(I)$] reflections	39962, 8552, 7393
R_{int}	0.047
(sin $\theta/\lambda)_{max}$ (Å^{-1})	0.666
Refinement	
$R[F^2 > 2\sigma(F^2)]$, $wR(F^2)$, S	0.036, 0.073, 1.04
No. of reflections	8552
No. of parameters	461
H-atom treatment	H-atom parameters constrained
$\Delta\rho_{max}$, $\Delta\rho_{min}$ (e Å^{-3})	0.41, −0.45

Computer programs: *COLLECT* (Nonius, 1998), *HKL-3000* (Otwinowski & Minor, 1997), *SHELXS97* (Sheldrick, 2008), *SHELXL2018/3* (Sheldrick, 2015), *ShelXle* (Hübschle *et al.*, 2011), *Mercury* (Macrae *et al.*, 2020), and *publCIF* (Westrip, 2010).

Funding information

Funding for this research was provided by the National Science Foundation (grant No. CHE-1625543 to M. Zeller; grants No. CHE-1465133 and CHE-1800361 to C. Brückner).

References

Albrecht, M., Burk, S. & Weis, P. (2008). *Synthesis*, pp. 2963–2967.
Albrecht, M., Chen, X. & Van Craen, D. (2019). *Chem. Eur. J.* **25**, 4265–4273.
Ali, N. J. & Milne, S. J. (1987). *British Ceram. Trans. J.* **86**, 113–117.
Alvarez, S., Avnir, D., Llunell, M. & Pinsky, M. (2002). *New J. Chem.* **26**, 996–1009.
Bazhenova, T. A., Kovaleva, N. V., Shilov, G. V., Petrova, G. N. & Kuznetsov, D. A. (2016). *Eur. J. Inorg. Chem.* pp. 5215–5221.
Bobbitt, N. S. & Snurr, R. Q. (2018). *Ind. Eng. Chem. Res.* **57**, 17488–17495.
Borgias, B. A., Cooper, S. R., Koh, Y. B. & Raymond, K. N. (1984). *Inorg. Chem.* **23**, 1009–1016.
Brückner, C., Powers, R. E. & Raymond, K. N. (1998). *Angew. Chem. Int. Ed.* **37**, 1837–1839.
Cao, J., Ma, W., Lyu, K., Zhuang, L., Cong, H. & Deng, H. (2020). *Chem. Sci.* **11**, 3978–3985.
Casanova, D., Cirera, J., Llunell, M., Alemany, P., Avnir, D. & Alvarez, S. (2004). *J. Am. Chem. Soc.* **126**, 1755–1763.
Caulder, D. L., Brückner, C., Powers, R. E., König, S., Parac, T. N., Leary, J. A. & Raymond, K. N. (2001). *J. Am. Chem. Soc.* **123**, 8923–8938.
Chen, X., Gerger, T. M., Räuber, C., Raabe, G., Göb, C., Oppel, I. M. & Albrecht, M. (2018). *Angew. Chem. Int. Ed.* **57**, 11817–11820.
Cirera, J., Ruiz, E. & Alvarez, S. (2005). *Organometallics*, **24**, 1556–1562.
Davies, J. A. & Dutremez, S. (1990). *J. Am. Ceram. Soc.* **73**, 1429–1430.
Davis, A. V., Firman, T. K., Hay, B. P. & Raymond, K. N. (2006). *J. Am. Chem. Soc.* **128**, 9484–9496.
Dehaen, G., Eliseeva, S. V., Kimpe, K., Laurent, S., Vander Elst, L., Muller, R. N., Dehaen, W., Binnemans, K. & Parac-Vogt, T. N. (2012). *Chem. Eur. J.* **18**, 293–302.
Dong, G.-L., Wang, L., Fang, W.-H. & Zhang, L. (2018). *Inorg. Chem. Commun.* **93**, 61–64.
Groom, C. R., Bruno, I. J., Lightfoot, M. P. & Ward, S. C. (2016). *Acta Cryst.* B**72**, 171–179.
Hahn, F. E., Rupprecht, S. & Moock, K. H. (1991). *J. Chem. Soc. Chem. Commun.* pp. 224–225.
Hübschle, C. B., Sheldrick, G. M. & Dittrich, B. (2011). *J. Appl. Cryst.* **44**, 1281–1284.

Johnson, S. H., Jackson, C. E. & Zadrozny, J. M. (2020). *Inorg. Chem.* **59**, 7479–7486.
Kaim, W. & Schwederski, B. (2010). *Coord. Chem. Rev.* **254**, 1580–1588.
Kwamen, A. C. N., Schlottmann, M., Van Craen, D., Isaak, E., Baums, J., Shen, L., Massomi, A., Räuber, C., Joseph, B. P., Raabe, G., Göb, C., Oppel, I. M., Puttreddy, R., Ward, J. S., Rissanen, K., Fröhlich, R. & Albrecht, M. (2020). *Chem. Eur. J.* **26**, 1396–1405.
Macrae, C. F., Sovago, I., Cottrell, S. J., Galek, P. T. A., McCabe, P., Pidcock, E., Platings, M., Shields, G. P., Stevens, J. S., Towler, M. & Wood, P. A. (2020). *J. Appl. Cryst.* **53**, 226–235.
Marteel-Parrish, A., DeCarlo, S., Harlan, D., Martin, J. & Sheridan, H. (2008). *Green Chem. Lett. Rev.* **1**, 197–203.
Nguyen, N. T. T., Furukawa, H., Gándara, F., Trickett, C. A., Jeong, H. M., Cordova, K. E. & Yaghi, O. M. (2015). *J. Am. Chem. Soc.* **137**, 15394–15397.
Nonius (1998). *COLLECT*. Nonius BV, Delft, The Netherlands.
Otwinowski, Z. & Minor, W. (1997). *Methods in Enzymology*, Vol. 276, *Macromolecular Crystallography*, Part A, edited by C. W. Carter Jr & R. M. Sweet, pp. 307–326. New York: Academic Press.
Passadis, S. S., Papanikolaou, M. G., Elliott, A., Tsiafoulis, C. G., Tsipis, A. C., Keramidas, A. D., Miras, H. N. & Kabanos, T. A. (2020). *Inorg. Chem.* **59**, 18345–18357.
Pierpont, C. G. & Lange, C. W. (1994). *Prog. Inorg. Chem.* **41**, 331–442.
Pinsky, M. & Avnir, D. (1998). *Inorg. Chem.* **37**, 5575–5582.
Sakata, Y., Hiraoka, S. & Shionoya, M. (2010). *Chem. Eur. J.* **16**, 3318–3325.
Sheldrick, G. M. (2008). *Acta Cryst.* A**64**, 112–122.
Sheldrick, G. M. (2015). *Acta Cryst.* C**71**, 3–8.
Sonström, A., Schneider, D., Maichle–Mössmer, C. & Anwander, R. (2019). *Eur. J. Inorg. Chem.* pp.682–692.
Tinoco, A. D., Eames, E. V., Incarvito, C. D. & Valentine, A. M. (2008). *Inorg. Chem.* **47**, 8380–8390.
Van Craen, D., Albrecht, M., Raabe, G., Pan, F. & Rissanen, K. (2016). *Chem. Eur. J.* **22**, 3255–3258.
Westrip, S. P. (2010). *J. Appl. Cryst.* **43**, 920–925.

supporting information

Acta Cryst. (2022). E**78**, 385-391 [https://doi.org/10.1107/S2056989022002638]

Bis(catecholato-κ^2O,O')bis(dimethyl sulfoxide-κO)titanium(IV)

Nisansala Hewage, Carolyn Mastriano, Christian Brückner and Matthias Zeller

Computing details

Data collection: *COLLECT* (Nonius, 1998); cell refinement: *HKL-3000* (Otwinowski & Minor, 1997); data reduction: *HKL-3000* (Otwinowski & Minor, 1997); program(s) used to solve structure: *SHELXS97* (Sheldrick, 2008); program(s) used to refine structure: *SHELXL2018/3* (Sheldrick, 2015), *ShelXle* (Hübschle *et al.*, 2011); molecular graphics: *Mercury* (Macrae *et al.*, 2020); software used to prepare material for publication: *publCIF* (Westrip, 2010).

Bis(benzene-1,2-diolato-κ^2O,O')bis(dimethyl sulfoxide-κO)titanium(IV)

Crystal data

$[Ti(C_6H_4O_2)_2(C_2H_6OS)_2]$
M_r = 420.34
Monoclinic, $P2_1/c$
a = 12.4531 (3) Å
b = 14.7287 (3) Å
c = 20.3676 (5) Å
β = 90.0445 (9)°
V = 3735.78 (15) Å^3
Z = 8
$F(000)$ = 1744
D_x = 1.495 Mg m^{-3}
Mo $K\alpha$ radiation, λ = 0.71073 Å
Cell parameters from 39962 reflections
θ = 1.4–28.3°
μ = 0.71 mm^{-1}
T = 100 K
Plate, orange
0.35 × 0.23 × 0.09 mm

Data collection

Nonius Kappa CCD diffractometer
Radiation source: fine focus X-ray tube
Graphite monochromator
ω and φ scans
Absorption correction: multi-scan (SCALEPACK; Otwinowski & Minor, 1997)
T_{min} = 0.668, T_{max} = 0.939
39962 measured reflections
8552 independent reflections
7393 reflections with $I > 2\sigma(I)$
R_{int} = 0.047
θ_{max} = 28.3°, θ_{min} = 1.4°
h = −16→14
k = −19→18
l = −25→27

Refinement

Refinement on F^2
Least-squares matrix: full
$R[F^2 > 2\sigma(F^2)]$ = 0.036
$wR(F^2)$ = 0.073
S = 1.04
8552 reflections
461 parameters
0 restraints
Primary atom site location: structure-invariant direct methods
Secondary atom site location: difference Fourier map
Hydrogen site location: inferred from neighbouring sites
H-atom parameters constrained
$w = 1/[\sigma^2(F_o^2) + (0.0246P)^2 + 2.3086P]$ where $P = (F_o^2 + 2F_c^2)/3$
$(\Delta/\sigma)_{max}$ = 0.001
$\Delta\rho_{max}$ = 0.41 e Å^{-3}
$\Delta\rho_{min}$ = −0.45 e Å^{-3}
Extinction correction: SHELXL2018/3 (Sheldrick 2015), $Fc^*=kFc[1+0.001xFc^2\lambda^3/\sin(2\theta)]^{-1/4}$
Extinction coefficient: 0.00192 (16)

Special details

Geometry. All esds (except the esd in the dihedral angle between two l.s. planes) are estimated using the full covariance matrix. The cell esds are taken into account individually in the estimation of esds in distances, angles and torsion angles; correlations between esds in cell parameters are only used when they are defined by crystal symmetry. An approximate (isotropic) treatment of cell esds is used for estimating esds involving l.s. planes.

Refinement. The structure exhibits pseudo-orthorhombic symmetry (Pbca) and is twinned by a 180 degree rotation around the a or c-axis. Application of the twin matrix 1 0 0, 0 -1 0, 0 0 -1 yielded a twin ratio of 0.5399 (7) to 0.4401 (7). The pseudo-orthorhombic symmetry is broken by modulation of the phenylene rings by up to 1.4 Angstrom.

Fractional atomic coordinates and isotropic or equivalent isotropic displacement parameters (Å²)

	x	*y*	*z*	U_{iso}*/U_{eq}
Ti1A	0.23792 (4)	0.86347 (3)	0.47159 (2)	0.01639 (11)
S1A	0.01041 (6)	0.90084 (4)	0.40944 (3)	0.01861 (14)
S2A	0.17900 (6)	0.65300 (4)	0.43411 (4)	0.02237 (15)
O1A	0.29396 (14)	0.97324 (11)	0.50941 (9)	0.0181 (4)
O2A	0.23951 (14)	0.82784 (11)	0.56301 (8)	0.0186 (4)
O3A	0.24928 (15)	0.89650 (11)	0.37882 (9)	0.0199 (4)
O4A	0.36941 (15)	0.80282 (12)	0.45119 (9)	0.0196 (4)
O5A	0.09197 (14)	0.92578 (12)	0.46412 (9)	0.0193 (4)
O6A	0.14803 (15)	0.75007 (12)	0.45420 (9)	0.0220 (4)
C1A	0.3082 (2)	0.97271 (16)	0.57562 (13)	0.0171 (5)
C2A	0.3488 (2)	1.04342 (17)	0.61292 (13)	0.0208 (5)
H2A	0.368091	1.099281	0.592823	0.025*
C3A	0.3608 (2)	1.03143 (19)	0.68025 (14)	0.0278 (6)
H3A	0.388467	1.079614	0.706268	0.033*
C4A	0.3331 (3)	0.9502 (2)	0.70978 (15)	0.0293 (7)
H4A	0.342127	0.943114	0.755821	0.035*
C5A	0.2919 (2)	0.87832 (18)	0.67256 (14)	0.0246 (6)
H5A	0.273006	0.822531	0.692909	0.030*
C6A	0.2790 (2)	0.89005 (17)	0.60499 (13)	0.0169 (5)
C7A	0.3287 (2)	0.85289 (16)	0.34636 (13)	0.0186 (5)
C8A	0.3427 (2)	0.85377 (18)	0.27873 (13)	0.0249 (6)
H8A	0.296315	0.887824	0.251048	0.030*
C9A	0.4274 (2)	0.80286 (19)	0.25277 (14)	0.0270 (6)
H9A	0.437837	0.801484	0.206588	0.032*
C10A	0.4962 (2)	0.75445 (18)	0.29301 (14)	0.0269 (6)
H10A	0.553816	0.721326	0.274072	0.032*
C11A	0.4823 (2)	0.75350 (17)	0.36086 (14)	0.0230 (6)
H11A	0.530330	0.721273	0.388597	0.028*
C12A	0.3960 (2)	0.80109 (17)	0.38657 (13)	0.0179 (5)
C13A	−0.0307 (2)	1.00875 (18)	0.37881 (14)	0.0231 (6)
H13A	−0.094276	1.001230	0.350983	0.035*
H13B	0.027660	1.035434	0.352935	0.035*
H13C	−0.047955	1.048911	0.415678	0.035*
C14A	−0.1055 (2)	0.86991 (17)	0.45376 (14)	0.0219 (6)
H14A	−0.165463	0.861017	0.423232	0.033*
H14B	−0.123587	0.918174	0.484975	0.033*

H14C	−0.091925	0.813351	0.477709	0.033*
C15A	0.1571 (3)	0.6507 (2)	0.34776 (16)	0.0470 (10)
H15A	0.164735	0.588285	0.331680	0.070*
H15B	0.209848	0.689715	0.325975	0.070*
H15C	0.084493	0.672688	0.338069	0.070*
C16A	0.0645 (2)	0.58991 (18)	0.45798 (15)	0.0267 (6)
H16A	0.069675	0.528144	0.440385	0.040*
H16B	−0.000313	0.619270	0.440775	0.040*
H16C	0.060692	0.587406	0.506008	0.040*
Ti1B	0.26978 (4)	0.36710 (3)	0.47110 (2)	0.01648 (10)
S1B	0.48538 (6)	0.41289 (4)	0.39989 (3)	0.01951 (14)
S2B	0.32921 (5)	0.15962 (4)	0.44898 (3)	0.01756 (14)
O1B	0.22436 (15)	0.46008 (11)	0.53031 (9)	0.0204 (4)
O2B	0.28384 (14)	0.30116 (11)	0.55326 (9)	0.0195 (4)
O3B	0.22962 (15)	0.41888 (11)	0.38620 (9)	0.0190 (4)
O4B	0.13334 (14)	0.30782 (12)	0.45810 (9)	0.0193 (4)
O5B	0.41145 (15)	0.43189 (12)	0.45889 (9)	0.0213 (4)
O6B	0.35320 (15)	0.26045 (11)	0.43304 (9)	0.0197 (4)
C1B	0.2044 (2)	0.43151 (18)	0.59244 (13)	0.0190 (5)
C2B	0.1564 (2)	0.48346 (19)	0.64125 (14)	0.0252 (6)
H2B	0.137199	0.544949	0.633482	0.030*
C3B	0.1374 (3)	0.4429 (2)	0.70182 (15)	0.0318 (7)
H3B	0.105239	0.477313	0.736001	0.038*
C4B	0.1645 (2)	0.3529 (2)	0.71306 (14)	0.0306 (7)
H4B	0.148461	0.325989	0.754284	0.037*
C5B	0.2149 (2)	0.30157 (19)	0.66489 (13)	0.0264 (6)
H5B	0.235155	0.240446	0.673191	0.032*
C6B	0.2353 (2)	0.34154 (17)	0.60413 (13)	0.0201 (5)
C7B	0.1430 (2)	0.38045 (16)	0.35732 (13)	0.0189 (6)
C8B	0.1074 (2)	0.39564 (18)	0.29362 (14)	0.0248 (6)
H8B	0.145005	0.435848	0.265315	0.030*
C9B	0.0150 (3)	0.35044 (19)	0.27199 (14)	0.0295 (6)
H9B	−0.009738	0.360043	0.228406	0.035*
C10B	−0.0408 (2)	0.29247 (18)	0.31242 (14)	0.0256 (6)
H10B	−0.103731	0.263272	0.296679	0.031*
C11B	−0.0054 (2)	0.27610 (17)	0.37675 (13)	0.0221 (6)
H11B	−0.043914	0.236415	0.404958	0.027*
C12B	0.0873 (2)	0.31931 (17)	0.39817 (13)	0.0176 (5)
C13B	0.5285 (3)	0.52345 (18)	0.37659 (15)	0.0271 (7)
H13D	0.584170	0.518513	0.342780	0.041*
H13E	0.557799	0.555009	0.414997	0.041*
H13F	0.467374	0.557725	0.359159	0.041*
C14B	0.6051 (2)	0.37109 (19)	0.43729 (16)	0.0274 (7)
H14D	0.659787	0.361118	0.403503	0.041*
H14E	0.589689	0.313647	0.459669	0.041*
H14F	0.631484	0.415538	0.469258	0.041*
C15B	0.2614 (2)	0.12076 (17)	0.37805 (14)	0.0271 (6)
H15D	0.250241	0.055054	0.381248	0.041*

H15E	0.304702	0.134322	0.339095	0.041*
H15F	0.191809	0.151379	0.374497	0.041*
C16B	0.4557 (2)	0.10696 (18)	0.43641 (15)	0.0243 (6)
H16D	0.447454	0.040889	0.439005	0.036*
H16E	0.506156	0.127350	0.470277	0.036*
H16F	0.483304	0.123567	0.392994	0.036*

Atomic displacement parameters (Å²)

	U^{11}	U^{22}	U^{33}	U^{12}	U^{13}	U^{23}
Ti1A	0.0163 (3)	0.0142 (2)	0.0187 (2)	0.00011 (18)	−0.0001 (2)	−0.00122 (16)
S1A	0.0179 (3)	0.0183 (3)	0.0196 (3)	0.0017 (2)	−0.0006 (3)	−0.0031 (2)
S2A	0.0197 (4)	0.0154 (3)	0.0319 (4)	−0.0009 (2)	0.0018 (3)	0.0002 (3)
O1A	0.0205 (10)	0.0161 (9)	0.0175 (9)	−0.0006 (7)	−0.0004 (7)	0.0008 (7)
O2A	0.0190 (10)	0.0166 (8)	0.0203 (9)	−0.0029 (7)	0.0006 (8)	−0.0004 (7)
O3A	0.0197 (10)	0.0204 (9)	0.0197 (9)	0.0040 (7)	−0.0002 (8)	0.0006 (7)
O4A	0.0210 (10)	0.0191 (9)	0.0188 (9)	0.0022 (7)	0.0007 (8)	0.0000 (7)
O5A	0.0159 (10)	0.0202 (9)	0.0218 (10)	0.0022 (7)	−0.0018 (8)	−0.0061 (8)
O6A	0.0213 (10)	0.0171 (9)	0.0276 (10)	−0.0012 (7)	−0.0001 (8)	−0.0050 (7)
C1A	0.0117 (13)	0.0177 (12)	0.0219 (13)	0.0041 (9)	0.0000 (10)	−0.0002 (10)
C2A	0.0173 (14)	0.0182 (12)	0.0271 (14)	−0.0019 (10)	−0.0020 (11)	−0.0010 (10)
C3A	0.0283 (16)	0.0273 (14)	0.0278 (15)	−0.0022 (11)	−0.0078 (13)	−0.0059 (12)
C4A	0.0307 (18)	0.0382 (17)	0.0190 (14)	−0.0020 (13)	−0.0057 (12)	−0.0028 (12)
C5A	0.0209 (15)	0.0271 (14)	0.0258 (15)	−0.0015 (11)	−0.0005 (12)	0.0052 (11)
C6A	0.0117 (13)	0.0180 (12)	0.0210 (13)	0.0007 (10)	−0.0013 (10)	−0.0019 (10)
C7A	0.0184 (15)	0.0159 (12)	0.0216 (13)	−0.0028 (10)	0.0029 (11)	−0.0005 (10)
C8A	0.0292 (17)	0.0238 (14)	0.0217 (14)	−0.0046 (11)	−0.0008 (12)	0.0023 (11)
C9A	0.0316 (17)	0.0285 (15)	0.0209 (15)	−0.0051 (12)	0.0087 (12)	−0.0040 (11)
C10A	0.0252 (15)	0.0231 (13)	0.0323 (16)	−0.0037 (12)	0.0075 (13)	−0.0041 (12)
C11A	0.0191 (15)	0.0178 (13)	0.0322 (15)	−0.0003 (11)	0.0035 (12)	−0.0019 (11)
C12A	0.0177 (14)	0.0158 (12)	0.0203 (14)	−0.0032 (10)	0.0017 (11)	−0.0010 (10)
C13A	0.0253 (16)	0.0236 (14)	0.0205 (15)	−0.0002 (11)	0.0004 (12)	0.0046 (11)
C14A	0.0199 (14)	0.0179 (13)	0.0280 (15)	0.0000 (10)	0.0008 (12)	0.0013 (11)
C15A	0.076 (3)	0.0343 (18)	0.0308 (18)	−0.0207 (17)	0.0158 (18)	−0.0095 (14)
C16A	0.0244 (15)	0.0186 (13)	0.0372 (17)	−0.0038 (11)	0.0053 (13)	−0.0019 (12)
Ti1B	0.0168 (2)	0.0141 (2)	0.0185 (2)	0.00012 (18)	0.0016 (2)	0.00020 (17)
S1B	0.0187 (3)	0.0180 (3)	0.0219 (3)	−0.0023 (3)	0.0019 (3)	−0.0018 (2)
S2B	0.0156 (3)	0.0140 (3)	0.0231 (3)	−0.0003 (2)	0.0016 (3)	0.0003 (2)
O1B	0.0216 (10)	0.0173 (8)	0.0224 (10)	0.0025 (7)	0.0018 (8)	0.0000 (7)
O2B	0.0204 (10)	0.0179 (9)	0.0202 (10)	0.0010 (7)	−0.0002 (8)	−0.0007 (7)
O3B	0.0204 (10)	0.0174 (8)	0.0193 (9)	−0.0031 (7)	0.0009 (8)	0.0014 (7)
O4B	0.0191 (10)	0.0207 (9)	0.0180 (9)	−0.0003 (7)	0.0006 (8)	0.0037 (7)
O5B	0.0206 (10)	0.0208 (10)	0.0226 (10)	−0.0010 (7)	0.0055 (9)	−0.0047 (8)
O6B	0.0205 (10)	0.0131 (8)	0.0256 (10)	−0.0024 (7)	0.0059 (8)	−0.0012 (7)
C1B	0.0168 (14)	0.0219 (13)	0.0182 (13)	−0.0019 (10)	0.0028 (10)	−0.0037 (10)
C2B	0.0211 (15)	0.0256 (14)	0.0289 (15)	0.0000 (11)	0.0003 (12)	−0.0067 (11)
C3B	0.0296 (18)	0.0444 (18)	0.0215 (15)	−0.0053 (14)	0.0052 (13)	−0.0102 (13)
C4B	0.0297 (17)	0.0444 (18)	0.0176 (14)	−0.0072 (13)	0.0008 (12)	−0.0036 (12)

C5B	0.0285 (16)	0.0293 (15)	0.0213 (14)	−0.0049 (11)	−0.0020 (12)	0.0026 (11)
C6B	0.0149 (13)	0.0254 (13)	0.0201 (13)	−0.0024 (10)	−0.0019 (11)	−0.0056 (11)
C7B	0.0215 (15)	0.0143 (12)	0.0210 (13)	0.0007 (10)	0.0011 (11)	−0.0016 (10)
C8B	0.0335 (17)	0.0217 (14)	0.0190 (14)	−0.0026 (11)	0.0032 (12)	0.0034 (11)
C9B	0.0386 (18)	0.0305 (15)	0.0195 (14)	−0.0009 (13)	−0.0054 (13)	−0.0029 (11)
C10B	0.0247 (16)	0.0260 (14)	0.0260 (15)	−0.0037 (11)	−0.0055 (12)	−0.0025 (11)
C11B	0.0211 (15)	0.0200 (13)	0.0252 (14)	−0.0020 (10)	0.0023 (12)	0.0002 (10)
C12B	0.0197 (14)	0.0164 (12)	0.0166 (13)	0.0030 (10)	0.0014 (11)	−0.0005 (10)
C13B	0.0288 (17)	0.0234 (14)	0.0290 (16)	−0.0050 (12)	−0.0016 (13)	0.0069 (12)
C14B	0.0231 (16)	0.0247 (15)	0.0344 (17)	0.0028 (11)	0.0018 (13)	0.0019 (13)
C15B	0.0273 (16)	0.0194 (13)	0.0347 (16)	−0.0006 (11)	−0.0076 (13)	−0.0025 (11)
C16B	0.0190 (15)	0.0219 (13)	0.0320 (16)	0.0024 (10)	0.0016 (12)	0.0026 (11)

Geometric parameters (Å, º)

Ti1A—O4A	1.9113 (19)	Ti1B—O1B	1.9108 (18)
Ti1A—O1A	1.9220 (17)	Ti1B—O4B	1.9284 (19)
Ti1A—O2A	1.9346 (18)	Ti1B—O2B	1.9427 (18)
Ti1A—O3A	1.9564 (18)	Ti1B—O3B	1.9545 (18)
Ti1A—O6A	2.0414 (18)	Ti1B—O5B	2.0214 (19)
Ti1A—O5A	2.0416 (18)	Ti1B—O6B	2.0367 (17)
S1A—O5A	1.5509 (19)	S1B—O5B	1.5400 (19)
S1A—C14A	1.763 (3)	S1B—C13B	1.779 (3)
S1A—C13A	1.782 (3)	S1B—C14B	1.783 (3)
S2A—O6A	1.5364 (19)	S2B—O6B	1.5494 (18)
S2A—C16A	1.771 (3)	S2B—C15B	1.768 (3)
S2A—C15A	1.780 (3)	S2B—C16B	1.774 (3)
O1A—C1A	1.360 (3)	O1B—C1B	1.357 (3)
O2A—C6A	1.346 (3)	O2B—C6B	1.339 (3)
O3A—C7A	1.352 (3)	O3B—C7B	1.353 (3)
O4A—C12A	1.358 (3)	O4B—C12B	1.359 (3)
C1A—C2A	1.384 (4)	C1B—C2B	1.390 (4)
C1A—C6A	1.404 (3)	C1B—C6B	1.400 (4)
C2A—C3A	1.391 (4)	C2B—C3B	1.392 (4)
C2A—H2A	0.9500	C2B—H2B	0.9500
C3A—C4A	1.383 (4)	C3B—C4B	1.387 (4)
C3A—H3A	0.9500	C3B—H3B	0.9500
C4A—C5A	1.399 (4)	C4B—C5B	1.389 (4)
C4A—H4A	0.9500	C4B—H4B	0.9500
C5A—C6A	1.396 (4)	C5B—C6B	1.394 (4)
C5A—H5A	0.9500	C5B—H5B	0.9500
C7A—C8A	1.389 (4)	C7B—C8B	1.389 (4)
C7A—C12A	1.398 (4)	C7B—C12B	1.409 (4)
C8A—C9A	1.398 (4)	C8B—C9B	1.401 (4)
C8A—H8A	0.9500	C8B—H8B	0.9500
C9A—C10A	1.383 (4)	C9B—C10B	1.375 (4)
C9A—H9A	0.9500	C9B—H9B	0.9500
C10A—C11A	1.393 (4)	C10B—C11B	1.403 (4)

C10A—H10A	0.9500	C10B—H10B	0.9500
C11A—C12A	1.385 (4)	C11B—C12B	1.388 (4)
C11A—H11A	0.9500	C11B—H11B	0.9500
C13A—H13A	0.9800	C13B—H13D	0.9800
C13A—H13B	0.9800	C13B—H13E	0.9800
C13A—H13C	0.9800	C13B—H13F	0.9800
C14A—H14A	0.9800	C14B—H14D	0.9800
C14A—H14B	0.9800	C14B—H14E	0.9800
C14A—H14C	0.9800	C14B—H14F	0.9800
C15A—H15A	0.9800	C15B—H15D	0.9800
C15A—H15B	0.9800	C15B—H15E	0.9800
C15A—H15C	0.9800	C15B—H15F	0.9800
C16A—H16A	0.9800	C16B—H16D	0.9800
C16A—H16B	0.9800	C16B—H16E	0.9800
C16A—H16C	0.9800	C16B—H16F	0.9800

O4A—Ti1A—O1A	99.75 (8)	O1B—Ti1B—O4B	98.62 (8)
O4A—Ti1A—O2A	94.27 (8)	O1B—Ti1B—O2B	80.85 (8)
O1A—Ti1A—O2A	80.73 (7)	O4B—Ti1B—O2B	88.32 (8)
O4A—Ti1A—O3A	81.00 (8)	O1B—Ti1B—O3B	101.72 (8)
O1A—Ti1A—O3A	98.71 (8)	O4B—Ti1B—O3B	80.24 (8)
O2A—Ti1A—O3A	175.09 (8)	O2B—Ti1B—O3B	168.52 (8)
O4A—Ti1A—O6A	92.85 (8)	O1B—Ti1B—O5B	89.89 (8)
O1A—Ti1A—O6A	163.08 (8)	O4B—Ti1B—O5B	165.00 (8)
O2A—Ti1A—O6A	87.15 (7)	O2B—Ti1B—O5B	105.30 (8)
O3A—Ti1A—O6A	94.35 (8)	O3B—Ti1B—O5B	85.97 (8)
O4A—Ti1A—O5A	163.07 (8)	O1B—Ti1B—O6B	160.77 (8)
O1A—Ti1A—O5A	88.55 (7)	O4B—Ti1B—O6B	92.76 (8)
O2A—Ti1A—O5A	101.66 (8)	O2B—Ti1B—O6B	84.07 (7)
O3A—Ti1A—O5A	83.18 (8)	O3B—Ti1B—O6B	95.42 (8)
O6A—Ti1A—O5A	82.35 (7)	O5B—Ti1B—O6B	82.64 (7)
O5A—S1A—C14A	103.27 (12)	O5B—S1B—C13B	102.87 (13)
O5A—S1A—C13A	103.16 (12)	O5B—S1B—C14B	103.27 (13)
C14A—S1A—C13A	100.06 (13)	C13B—S1B—C14B	100.22 (14)
O6A—S2A—C16A	102.29 (12)	O6B—S2B—C15B	103.36 (12)
O6A—S2A—C15A	104.06 (14)	O6B—S2B—C16B	102.56 (12)
C16A—S2A—C15A	97.94 (16)	C15B—S2B—C16B	99.43 (14)
C1A—O1A—Ti1A	116.08 (15)	C1B—O1B—Ti1B	114.90 (15)
C6A—O2A—Ti1A	115.48 (15)	C6B—O2B—Ti1B	113.83 (15)
C7A—O3A—Ti1A	114.05 (15)	C7B—O3B—Ti1B	115.14 (15)
C12A—O4A—Ti1A	115.43 (16)	C12B—O4B—Ti1B	115.97 (16)
S1A—O5A—Ti1A	121.98 (10)	S1B—O5B—Ti1B	122.18 (11)
S2A—O6A—Ti1A	132.05 (11)	S2B—O6B—Ti1B	124.13 (11)
O1A—C1A—C2A	125.9 (2)	O1B—C1B—C2B	125.1 (2)
O1A—C1A—C6A	113.2 (2)	O1B—C1B—C6B	113.7 (2)
C2A—C1A—C6A	120.8 (2)	C2B—C1B—C6B	121.2 (2)
C1A—C2A—C3A	119.0 (2)	C1B—C2B—C3B	118.1 (3)
C1A—C2A—H2A	120.5	C1B—C2B—H2B	120.9

C3A—C2A—H2A	120.5	C3B—C2B—H2B	120.9
C4A—C3A—C2A	120.8 (3)	C4B—C3B—C2B	121.0 (3)
C4A—C3A—H3A	119.6	C4B—C3B—H3B	119.5
C2A—C3A—H3A	119.6	C2B—C3B—H3B	119.5
C3A—C4A—C5A	120.7 (3)	C3B—C4B—C5B	120.9 (3)
C3A—C4A—H4A	119.7	C3B—C4B—H4B	119.5
C5A—C4A—H4A	119.7	C5B—C4B—H4B	119.5
C6A—C5A—C4A	118.8 (3)	C4B—C5B—C6B	118.7 (3)
C6A—C5A—H5A	120.6	C4B—C5B—H5B	120.7
C4A—C5A—H5A	120.6	C6B—C5B—H5B	120.7
O2A—C6A—C5A	125.7 (2)	O2B—C6B—C5B	125.6 (2)
O2A—C6A—C1A	114.5 (2)	O2B—C6B—C1B	114.4 (2)
C5A—C6A—C1A	119.9 (2)	C5B—C6B—C1B	120.0 (2)
O3A—C7A—C8A	125.0 (2)	O3B—C7B—C8B	126.3 (2)
O3A—C7A—C12A	114.3 (2)	O3B—C7B—C12B	113.8 (2)
C8A—C7A—C12A	120.7 (3)	C8B—C7B—C12B	119.9 (2)
C7A—C8A—C9A	117.7 (3)	C7B—C8B—C9B	118.6 (2)
C7A—C8A—H8A	121.1	C7B—C8B—H8B	120.7
C9A—C8A—H8A	121.1	C9B—C8B—H8B	120.7
C10A—C9A—C8A	121.3 (3)	C10B—C9B—C8B	121.5 (3)
C10A—C9A—H9A	119.3	C10B—C9B—H9B	119.3
C8A—C9A—H9A	119.3	C8B—C9B—H9B	119.3
C9A—C10A—C11A	121.0 (3)	C9B—C10B—C11B	120.5 (3)
C9A—C10A—H10A	119.5	C9B—C10B—H10B	119.7
C11A—C10A—H10A	119.5	C11B—C10B—H10B	119.7
C12A—C11A—C10A	117.8 (3)	C12B—C11B—C10B	118.4 (2)
C12A—C11A—H11A	121.1	C12B—C11B—H11B	120.8
C10A—C11A—H11A	121.1	C10B—C11B—H11B	120.8
O4A—C12A—C11A	124.5 (2)	O4B—C12B—C11B	125.1 (2)
O4A—C12A—C7A	114.3 (2)	O4B—C12B—C7B	113.8 (2)
C11A—C12A—C7A	121.3 (3)	C11B—C12B—C7B	121.1 (2)
S1A—C13A—H13A	109.5	S1B—C13B—H13D	109.5
S1A—C13A—H13B	109.5	S1B—C13B—H13E	109.5
H13A—C13A—H13B	109.5	H13D—C13B—H13E	109.5
S1A—C13A—H13C	109.5	S1B—C13B—H13F	109.5
H13A—C13A—H13C	109.5	H13D—C13B—H13F	109.5
H13B—C13A—H13C	109.5	H13E—C13B—H13F	109.5
S1A—C14A—H14A	109.5	S1B—C14B—H14D	109.5
S1A—C14A—H14B	109.5	S1B—C14B—H14E	109.5
H14A—C14A—H14B	109.5	H14D—C14B—H14E	109.5
S1A—C14A—H14C	109.5	S1B—C14B—H14F	109.5
H14A—C14A—H14C	109.5	H14D—C14B—H14F	109.5
H14B—C14A—H14C	109.5	H14E—C14B—H14F	109.5
S2A—C15A—H15A	109.5	S2B—C15B—H15D	109.5
S2A—C15A—H15B	109.5	S2B—C15B—H15E	109.5
H15A—C15A—H15B	109.5	H15D—C15B—H15E	109.5
S2A—C15A—H15C	109.5	S2B—C15B—H15F	109.5
H15A—C15A—H15C	109.5	H15D—C15B—H15F	109.5

H15B—C15A—H15C	109.5	H15E—C15B—H15F	109.5
S2A—C16A—H16A	109.5	S2B—C16B—H16D	109.5
S2A—C16A—H16B	109.5	S2B—C16B—H16E	109.5
H16A—C16A—H16B	109.5	H16D—C16B—H16E	109.5
S2A—C16A—H16C	109.5	S2B—C16B—H16F	109.5
H16A—C16A—H16C	109.5	H16D—C16B—H16F	109.5
H16B—C16A—H16C	109.5	H16E—C16B—H16F	109.5

C14A—S1A—O5A—Ti1A	123.30 (13)	C13B—S1B—O5B—Ti1B	137.68 (14)
C13A—S1A—O5A—Ti1A	−132.84 (14)	C14B—S1B—O5B—Ti1B	−118.38 (14)
C16A—S2A—O6A—Ti1A	159.79 (16)	C15B—S2B—O6B—Ti1B	103.47 (15)
C15A—S2A—O6A—Ti1A	−98.66 (19)	C16B—S2B—O6B—Ti1B	−153.50 (14)
Ti1A—O1A—C1A—C2A	179.0 (2)	Ti1B—O1B—C1B—C2B	−170.4 (2)
Ti1A—O1A—C1A—C6A	0.2 (3)	Ti1B—O1B—C1B—C6B	8.6 (3)
O1A—C1A—C2A—C3A	−178.5 (3)	O1B—C1B—C2B—C3B	177.3 (3)
C6A—C1A—C2A—C3A	0.3 (4)	C6B—C1B—C2B—C3B	−1.6 (4)
C1A—C2A—C3A—C4A	0.1 (4)	C1B—C2B—C3B—C4B	−0.6 (4)
C2A—C3A—C4A—C5A	−0.2 (5)	C2B—C3B—C4B—C5B	2.2 (5)
C3A—C4A—C5A—C6A	−0.1 (4)	C3B—C4B—C5B—C6B	−1.7 (4)
Ti1A—O2A—C6A—C5A	−177.4 (2)	Ti1B—O2B—C6B—C5B	166.9 (2)
Ti1A—O2A—C6A—C1A	2.8 (3)	Ti1B—O2B—C6B—C1B	−13.3 (3)
C4A—C5A—C6A—O2A	−179.2 (3)	C4B—C5B—C6B—O2B	179.4 (3)
C4A—C5A—C6A—C1A	0.5 (4)	C4B—C5B—C6B—C1B	−0.4 (4)
O1A—C1A—C6A—O2A	−1.9 (3)	O1B—C1B—C6B—O2B	3.2 (3)
C2A—C1A—C6A—O2A	179.2 (2)	C2B—C1B—C6B—O2B	−177.7 (2)
O1A—C1A—C6A—C5A	178.3 (2)	O1B—C1B—C6B—C5B	−176.9 (2)
C2A—C1A—C6A—C5A	−0.6 (4)	C2B—C1B—C6B—C5B	2.1 (4)
Ti1A—O3A—C7A—C8A	169.6 (2)	Ti1B—O3B—C7B—C8B	−170.3 (2)
Ti1A—O3A—C7A—C12A	−7.5 (3)	Ti1B—O3B—C7B—C12B	9.2 (3)
O3A—C7A—C8A—C9A	−178.2 (2)	O3B—C7B—C8B—C9B	−179.3 (3)
C12A—C7A—C8A—C9A	−1.3 (4)	C12B—C7B—C8B—C9B	1.2 (4)
C7A—C8A—C9A—C10A	−1.1 (4)	C7B—C8B—C9B—C10B	0.4 (4)
C8A—C9A—C10A—C11A	1.1 (4)	C8B—C9B—C10B—C11B	−0.8 (4)
C9A—C10A—C11A—C12A	1.3 (4)	C9B—C10B—C11B—C12B	−0.4 (4)
Ti1A—O4A—C12A—C11A	−173.6 (2)	Ti1B—O4B—C12B—C11B	173.9 (2)
Ti1A—O4A—C12A—C7A	6.8 (3)	Ti1B—O4B—C12B—C7B	−5.8 (3)
C10A—C11A—C12A—O4A	176.7 (2)	C10B—C11B—C12B—O4B	−177.6 (2)
C10A—C11A—C12A—C7A	−3.7 (4)	C10B—C11B—C12B—C7B	2.0 (4)
O3A—C7A—C12A—O4A	0.6 (3)	O3B—C7B—C12B—O4B	−2.3 (3)
C8A—C7A—C12A—O4A	−176.6 (2)	C8B—C7B—C12B—O4B	177.2 (2)
O3A—C7A—C12A—C11A	−179.0 (2)	O3B—C7B—C12B—C11B	178.0 (2)
C8A—C7A—C12A—C11A	3.8 (4)	C8B—C7B—C12B—C11B	−2.4 (4)

Hydrogen-bond geometry (Å, º)

D—H···*A*	*D*—H	H···*A*	*D*···*A*	*D*—H···*A*
C11*A*—H11*A*···O2*B*^{i}	0.95	2.62	3.491 (3)	153
C13*A*—H13*C*···O5*A*^{ii}	0.98	2.54	3.428 (3)	151

C14*A*—H14*B*···O1*A*^{ii}	0.98	2.66	3.378 (3)	130
C14*A*—H14*B*···O5*A*^{ii}	0.98	2.55	3.447 (3)	152
C14*A*—H14*C*···O4*B*^{iii}	0.98	2.27	3.193 (3)	156
C13*B*—H13*E*···O5*B*^{i}	0.98	2.60	3.495 (4)	151
C14*B*—H14*E*···O4*A*^{i}	0.98	2.55	3.438 (3)	151
C14*B*—H14*F*···O1*B*^{i}	0.98	2.56	3.336 (3)	136
C15*B*—H15*D*···O3*A*^{iv}	0.98	2.34	3.307 (3)	171
C16*B*—H16*D*···O1*A*^{iv}	0.98	2.59	3.186 (3)	119
C16*B*—H16*E*···O4*A*^{i}	0.98	2.45	3.427 (3)	173

Symmetry codes: (i) −*x*+1, −*y*+1, −*z*+1; (ii) −*x*, −*y*+2, −*z*+1; (iii) −*x*, −*y*+1, −*z*+1; (iv) *x*, *y*−1, *z*.